doi:10.1017/S1431927620023053

Microsc. Microanal. 26 (Suppl 2), 2020

Low Dose HRTEM of Interfacial Melting of Cubic Ice at Low Temperature

Jianguo Wen, Yulin Lin, Xiao-Min Lin and Aiwen Lei

Argonne National Laboratory, Lemont, Illinois, United States

Four phases of ice show exist in outer space: hexagonal ice (ice I_h), cubic ice (ice I_c), amorphous ice, and orthorhombic ice (ice XI), which play crucially important roles in the origin of life. The environment in a cryogenic transmission electron microscope (cryo-TEM) with high vacuum and low temperature environment is very similar to outer space, which offers a unique way to investigate the behaviors of interstellar ice. Previously, Kobayashi et al. [1] directly observed hexagonal ice nanoparticles at atomic scale using aberration-corrected cryo-TEM. However, the atomic structure of cubic ice has not been fully understood yet because cubic ice is extremely sensitive to e-beam irradiation compared to hexagonal ice. By using low-temperature, low-dose high-resolution TEM (HRTEM) enabled by a direct electron detection camera, we demonstrate in situ atomic resolution observation of cubic ice melting. We found that ice, at the interface between ice film and substrates, melts into glass water (a melted amorphous ice) under the electron beam irradiation even at liquid nitrogen temperature.

Cubic ice is obtained by condensing residual water vapor to a cold amorphous carbon film on TEM grids in the electron microscope. **Fig. 1(a)** shows a typical STEM image of a cubic ice thin film formed at a temperature of 120 K, showing ice nanoparticles with an average diameter of 30 nm. SAED pattern in **Fig. 1(b)** is indexed as a cubic ice structure. Under a low-dose rate (~10^3 $e^-/^2s$) imaging condition, we are able to obtain atomic resolution HRTEM image a cubic ice without any stacking faults as shown in **Fig. 1(c)**. Ice formed by condensing water vapor on a cold support was not pure cubic ice [2], which always associated with stacking fault during the crystal growth. **Fig. 1(d)** shows such a mixed ice with numerous stacking faults.

Electron beam irradiation causes various phase transition of cubic ice. In addition, we found cubic ice melts into glass water and forms bubble at the interface between ice and substrate as shown in a schematic in **Fig. 2(a)** even at low temperature of ~100K. As shown in a TEM image in **Fig. 2(b)**, 10-100 nm nanobubbles appear randomly under the electron bean irradiation. Before the bubble formation in **Fig. 2(c)**, a clear diffraction contrast of ice film is observed. With the increasing of e-beam irradiation, nanobubbles start to grow and merge into bigger bubbles in **Fig. 2(d-f)**. The coalescing nanobubbles (marked by yellow circles) and Ostwald-ripening nanobubbles (marked by red circles) indicate that the ice melts into glass water with lower viscosity [3]. The intensity ratio between peak III and II in the O-K edge EELS spectra in **Fig. 2(k)** gradually decreases during melting, indicates an increase of glassy water near the final stage of ice melting [4].

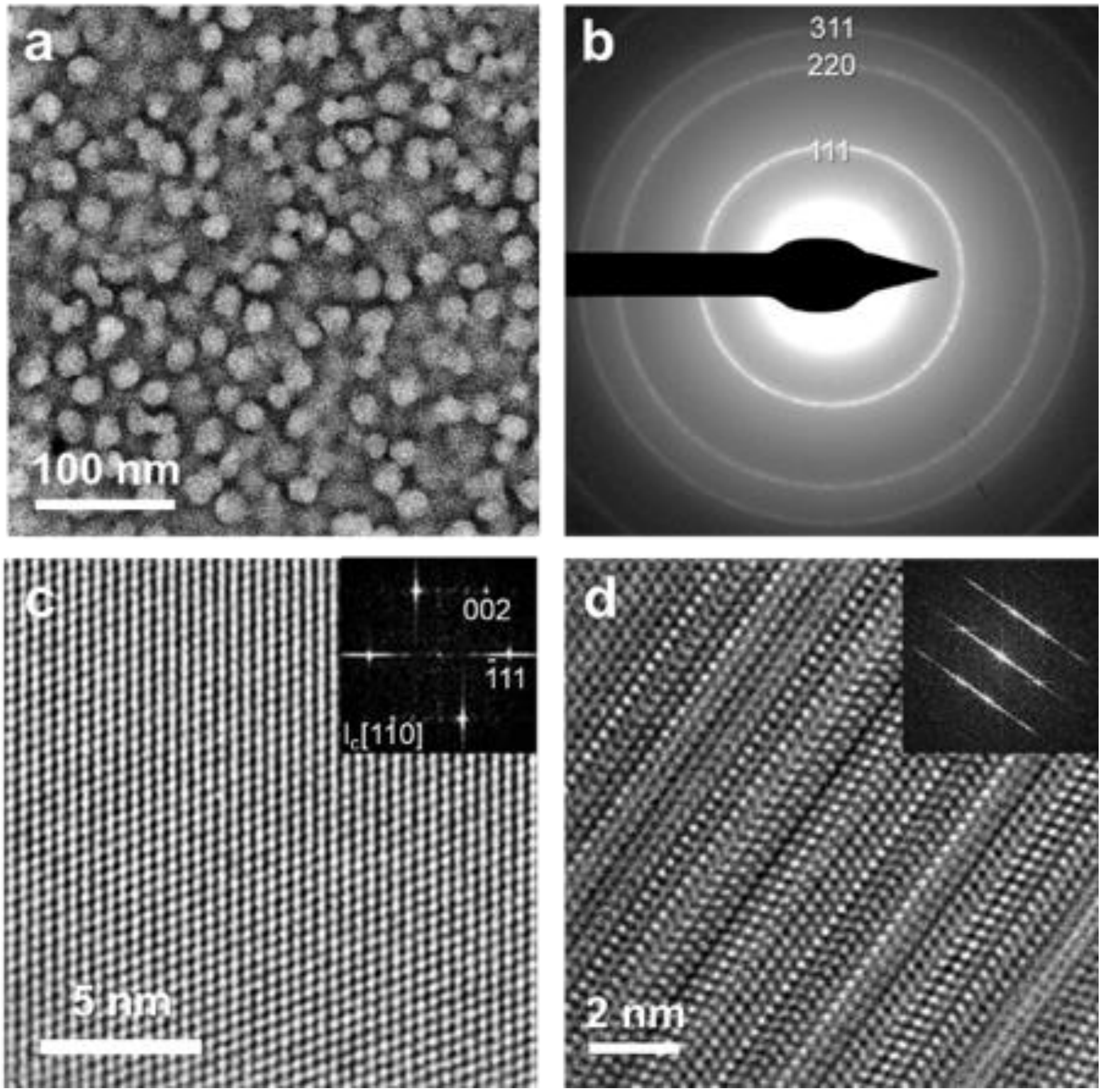

Figure 1. (a) STEM-HADDF image of cubic ice nano particles. (b) Typical SAED pattern of the ice thin film. (c) HRTEM and corresponding FFT pattern of a pure cubic ice nanoparticle. (d) HRTEM and corresponding FFT pattern of a mixed ice nanoparticle with stacking faults.

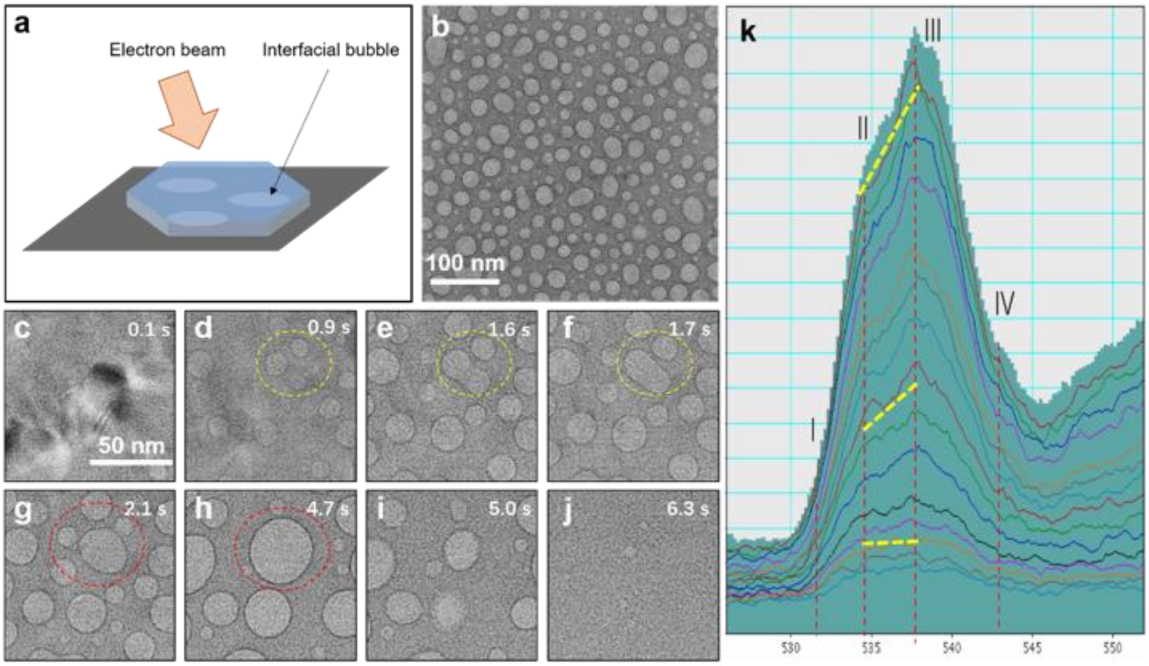

Figure 2. (a) a schematic of cubic ice interfacial melting under electron beam irradiation. (b) Low mag TEM images of nanobubbles. (c-j) The snap shots of TEM images showing the time evolution of nanobubbles. (k) Oxygen core-loss spectra of cubic ice melting.

References
[1] Kobayashi, K., Koshino, M., Suenaga, K., Physical Review Letters, 106(20), 206101(2011).
[2] Kuhs, W. F., Sippel, C., Falenty, A., & Hansen, T. C., Proceedings of the National Academy of Sciences, 109(52), 21259-21264(2012).
[3] Shin D, Park J B, Kim Y J, et al., Nature Communications, 6(1): 1-6(2015).
[4] This work was performed at the Center for Nanoscale Materials, a U.S. Department of Energy Office of Science User Facility, and supported by the U.S. Department of Energy, Office of Science, under Contract No. DE-AC02-06CH11357. This research is also supported by the National Natural Science Foundation of China (21520102003) and the Hubei Province Natural Science Foundation of China (2017CFA010). Yulin Lin is grateful for the Fundamental Research Funds for the Central Universities, China Scholarship Council (No 201706270411), and technical support from Dr. Guanyu Wang and Dr. Duan Luo.